Journal of Animal & Plant Sciences, 34(3): 2024, Page: 768-779
ISSN (print): 1018-7081; ISSN (online): 2309-8694
https://doi.org/10.36899/JAPS.2024.3.0763

TRANSCRIPTOME ANALYSIS OF FLOWER BUDS AT THREE DIFFERENT DEVELOPMENTAL STAGES IN *Cymbidium kanran*

L. Weiyi, L. Shaofan, W. Xinchen, Y. Boyun and L. Huolin*

School of Life Science, Nanchang University, Nanchang 330031, Jiangxi, China
*Corresponding Author's E-mail: 572460991@163.com

ABSTRACT

Cymbidium kanran is extensively cultivated and globally coveted, enjoying widespread popularity in horticulture circles. Despite its popularity, the intricate mechanisms underlying its flowering cycle have remained largely enigmatic. In this study, we conducted transcriptome sequencing on flower buds at three distinct stages, including the initiation of flower bud differentiation, the differentiation stage of flower primordium, and the stage of flower bud formation. This investigation aimed to unravel the flowering mechanism of the target species. Differential gene expression was screened and subjected to pathway enrichment analysis to identify key pathways involved in flowering regulation. Subsequently, the identified differentially expressed genes within these critical pathways were validated using RT-qPCR. The results showed that a total of 23720 differentially expressed genes (DEGs) were obtained. Through Gene Ontology (GO) functional annotation, it was found that it involved three categories of cellular component, biological process and molecular function, including 46 subcategories. Kyoto Encyclopedia of Genes and Genomes (KEGG) pathway enrichment analysis found that it was mainly enriched in metabolic pathways and biosynthetic of secondary metabolites pathways. In addition, this study found 29 genes related to four flowering regulatory pathways and flowering integration, including a gene related to autonomic pathway, five genes related to vernalization pathway, 13 genes related photoperiod pathway, four genes related to gibberellin (GA) pathway, and six genes related to flowering integration. Through RT-qPCR analyses, it was found that the relative expression of genes in RNA-seq was accurate and reliable. This study preliminarily revealed the molecular mechanism of flowering in *C. kanran*, and the results laid a foundation for the molecular regulation mechanism of flowering in *C. kanran*, and also provided a basis for the regulation of flowering period of orchids.

Key words: *Cymbidium kanran*; transcriptome; flowering regulation; differentially expressed gene

Published first online April 15, 2024 Published final May 31, 2024

INTRODUCTION

Cymbidium kanran (Orchidaceae) is a perennial herb, mainly distributed in the southern provinces of China, as well as southern Japan and the southern tip of the Korean Peninsula (Jeong *et al.,* 2017). It is a highly valued member of the orchid family due to its diverse lip shape variation, rich flower color, four-season flowering and long flowering period, and extremely high ornamental and economic value (Jian and Zhu, 2010). However, orchids, including *C. kanran*, take a very long time from seed germination to flowering, which seriously hinders related research on orchid flower development and orchid breeding (Yu *et al*., 2001). Therefore, studying the regulatory mechanism of flower bud differentiation in this species is of significant importance.

The differentiation of flower buds is a complex response process to signals from both external environmental and internal factors (Crane *et al.,* 2012). In the model plant *Arabidopsis thaliana*, multiple genes regulating the transition to flowering have been identified, primarily involving six regulatory pathways: vernalization, photoperiod, gibberellin, sugar metabolism, autonomous, and aging pathways (Blümel *et al.,* 2015). These pathways mediate and integrate the expression of flowering-related genes, such as FLOWER LOCUS T (*FT*), CONSTANS (*CO*), FLOWERING LOCUS C (*FLC*), SUPPRESSOR OF CO1 (*SOC1*), LEAFY *(LFY*), APETALA1 (*AP1*), AGAMOUS (*AG*), APETALA2 (*AP2*), and APETALA3 (*AP3*), irreversibly inducing the transformation of plants from vegetative growth tissues to reproductive growth tissues, playing a crucial role in the regulation of flower bud differentiation in angiosperms (Liu *et al.,* 2015). *FLC* acts as a flowering repressor, mediating vernalization and autonomous pathways, while *CO* acts as an activator and mediates the photoperiod pathway; both genes regulate the downstream expression of *FT*, *SOC1*, and *LFY* (Anders and Coupland, 2012). The *FT* protein complex activates characteristic genes *LFY* and *AP1* in reproductive tissues, controlling the

transition from vegetative to reproductive growth (Ferrandiz *et al.,* 2000; Fornara *et al.,* 2010). Flower organ characteristic genes such as *AP2*, *AP3*, and *AG* induce flower organ development under the control of MADS-box transcription factors (Theißen *et al.,* 2016). Additionally, plant hormones respond to environmental changes, regulate internal nutrient allocation, and even directly control the expression of flowering genes (Zou *et al*. 2020), closely related to flower bud differentiation. Auxin is involved in flower primordium differentiation by regulating *LFY* (Yamaguchi *et al.,* 2014), low IAA content promotes flower bud differentiation in 'Kyoho' grapes (Lin *et al.,* 2012), but leads to poor flower bud formation in 'Summer Black' grapes (Wang *et al.,* 2014). GAs participates in various plant developmental processes, including the initiation of flowering transition, flower primordium, and flower organ development (Binenbuam *et al.,* 2018). In *Arabidopsis*, GAs induce flowering by regulating floral integrators *SOC1* and *FT*, as well as the floral organ characteristic gene *LFY* (Jing *et al.,* 2020), while in some plants, it can inhibit flowering, such as in roses (Díaz-Riquelme *et al.,* 2014). ABA is a hormone signal that initiates fruit ripening and also plays an important role in flower bud differentiation (Chen *et al.,* 2018). ABA mainly affects the downstream *FT* expression activated by CO transcription (Conti *et al.,* 2017), and high concentrations are favorable for the bud differentiation of lychee (Cui *et al.,* 2013).

While some studies have reported on the flower bud differentiation of orchid plants, they have primarily focused on morphological and physiological information, and the regulatory mechanisms during the process of flower bud differentiation have not been fully elucidated (Feng *et al.,* 2021). RNA-seq can achieve synchronous analysis of transcripts and differentially expressed genes. Its results can accurately identify gene expression within a dynamic range, quickly identify differentially expressed genes, and perform more sensitive and accurate analysis of transcriptomes, thereby better understanding molecular mechanisms. Digital gene expression profiling (DGE) combines second-generation high-throughput sequencing with high-performance computing to obtain all gene expression data of a certain tissue at a high speed (Huang *et al.,* 2022; Wilhelm and Landry, 2009; Chen *et al.,* 2012). Building upon the established morphological changes during flower bud differentiation in *C. kanran* (Zhu *et al.,* 2008; Jiang, 2007), this study conducted high-throughput transcriptome sequencing analysis at three developmental stages of flower bud differentiation, including the initiation of flower bud differentiation, the differentiation stage of flower primordium, and the stage of flower bud formation. The aim is to discover genes potentially involved in flower bud differentiation and lay the foundation for understanding the regulatory mechanisms of flower bud differentiation in *C. kanran*.

MATERIALS AND METHODS

Plant materials: The *C. kanran* seedlings derived from tissue culture were cultivated in the orchid greenhouse at Nanchang University under conditions of 16 hours of light at 25℃ and 8 hours of darkness at 18℃. The relative humidity was maintained at 75% to 85%. From May to October of the 5th year of cultivation, flower buds at three developmental stages - the initiation of flower bud differentiation (F0), the differentiation stage of flower primordium (F1), and the flower bud formation stage (F2) were collected, coupled with anatomical observations. The excised flower bud tissues were rapidly frozen in liquid nitrogen and stored in a -80℃ freezer, with three biological replicates performed.

RNA Extraction and Transcriptome Sequencing: Total RNA was extracted from the samples using the Plant RNA Extraction Kit (QIAGEN, Germany), and the integrity and total amount of RNA were accurately detected using the Agilent 2100 Bioanalyzer. mRNA was enriched using magnetic beads with Oligo (dT), followed by fragmentation into short segments. cDNA was then constructed using these mRNA fragments as templates. After constructing the sequencing library, Illumina HiSeq was used for sequencing, ultimately obtaining raw sequencing data for the transcriptome.

Screening and enrichment analysis of differentially expressed genes: The construction and sequencing of the library implemented by Beijing Genomics Institute (BGI). The raw sequencing data was quality-controlled and adapter sequences, low-quality bases, and N bases were removed using the Trimmomatic-0.39 software to obtain high-quality reads. The gene expression levels were quantified using the cufflinks software, expressed as fragments per kilobase of exon model per million mapped fragments (FPKM). To calculate gene expression differences, htseq-count (2.0.3) software was used to count the number of reads for each gene in each sample. The data was normalized using the estimate Size Factors function from the DESeq (2012) R package, and the binom Test function was used to calculate the P-values and fold changes. Differential genes with $P < 0.05$ and a fold change > 2 were selected for GO and KEGG enrichment analysis to determine the main biological functions or pathways affected by the differential genes.

Validation of differentially expressed genes by RT-qPCR: RT-qPCR was performed using an CFX Connect™ Real-Time PCR Detection System and a TB Green® Premix Ex TaqTM II Kit. The RT-qPCR reaction was carried out in a 20 uL reaction, including 1.6 µl of cDNA, 0.8 µl of each primer (10 µM) (Table 1), and 10.0 µl of 2×TB Green Premix Ex Taq II (Tli RNaseH Plus). In addition, reactions without template or primer were used as a negative control to exclude possible

contamination. The thermal cycle program was set as the initial polymerase activation step, which was carried out for 30 s at 95℃, and then 40 cycles, including 15 s at 94℃ for template denaturation, 15 s at 55-65℃ for annealing, and 45 s at 72℃ for extension and fluorescence detection. All samples were amplified in triplicate. The specificity of RT-qPCR was confirmed by agarose electrophoresis and dissociation curve analysis. The cycle threshold for each reaction (Cq, the first cycle of the signal over the background) was automatically determined, by default parameters of the CFX Connect™ Real-Time PCR Detection System device.

Table 1. Primers for RT-qPCR analysis

Gene	Forward Primers (5'-3')	Reverse Primers (5'-3')
CkFPA	TTGTGAAGCATTTGGAGCAG	CATTGCAGCGAGATGACAGT
CkGA2OX	TCCATGCTTTGATTGTGGAA	ACCAAACCCAAACTGTCTGC
CkGID1	TTGAGGGAGGTTCAATTTGG	AGCCGTTTTCAACCATGAAC
CkGA20OX	GAAGAAGGGGATGGAGAACC	CTCTCACCGTCCTCTTCCAG
CkGA3OX	CCCACCTGCTATCCCACTAA	AGAAGGAGGAGCTTGGAAGG
CkCO	CCACAATTCCCTCTTCTCCA	ATTGATATATCCCGGCGTCA
CkGI	TGGAGTGCAGTTGAATCTCG	TGCATCTATGGCTGACTTGC
CkPHYA	CTGGCTAGTGGCAGTGATGA	GCAGAGCCAAAGGTCAAAAG
CkPHYB	TCAAGCCTCTCGGTTTCTGT	GGGGCAATTTTGGATTACCT
CkCRY	ACAAGAGAGCCACAGCCAGT	AAGGGCGTGATGTTTTTGAG
CkCRY1	CCCGTCCACCACGATATAAA	GGTGCTAGAACGAGGCTCAC
CkCRY2	GGGACCTGAGGATTGAGGAT	CCGGGATAGAACTTCCCTTC
CkUVR8	CTGGGAGACTTGGTCATGGT	ACACCAACAGCCTTTTCACC
CkCCA1	GCTCCTCCAACAAGCAGAAC	GTCAGTCGATTCTGCGACAA
CkLHY	GATGAACTGCCGGATTCTGT	GCCTAACCAACCACTTTCCA
CkDOF5	GATTCTGAGCACCGTTCCAT	CTGCAGTAGCAAGGACACCA
CkFKF1	GAGAGAGATGGGCGTCAAAG	CTTTCCCTTCTCCCACTTCC
CkELF3	TCATTCGATGGAGTGGTTTG	GTGGTTGACGATGGTGAGG
CkVIN3	AATTTCAGGGGCATTGTCTG	GATCCTGCAAAATGCAATGA
CkVRN	TGTTTGTCTGCTGAGGATGC	TGAAGCAGCCAGTTGTTGTC
CkELF4	CAATGTGGGGCTGATAAAGG	CGACCTGAACCTCTTCTTCG
CkFRI	TGAGCAGAAACTCACGGTTG	AACAGCAGGGATCAATTTGG
CkFLC	GGTTGAATTTTCCAGCCAGA	GCAGTCTGGCATTCAGAACA
CkFT	GGACAATTGCTACCCGAAAA	GTGTGGAGGATTGTGTGCTG
CkSOC1	AAAACCTGGAGTCCTGCTCA	CCTTGCTCGAGTTGACCTTC
CkAP1	TGACCAAGAGCTGTCGAAGA	GCATGAGCTCTCCATCCTCT
CkAGL6-2	TTTTCTTCTTGCGAGCCATT	TGCCTCGTAACTCCGTTTCT
CkAGL6-1	GCCGAACTCATAGAGCTTGC	CGCAGAGGTAGCCCTAATCA
CkAGL8	GTCTTTTGGCGTGGTGTTTT	AATTACCTCCCTTCGCCAAT

RESULTS

Transcriptome sequencing results and quality assessment: Flower buds of *C. kanran* at different stages, including flower bud initiation stage (F0), flower primordium differentiation stage (F1) and flower bud formation stage (F2), were used for RNA-seq, and three transcriptome databases were obtained. The total number of reads obtained in F0, F1 and F2 sequencing was 23625162, 22767464 and 23948875, respectively. The percentages of total mapped reads compared to All-Unigene were 79.57%, 79.85% and 82.27%, respectively, of which unique match accounted for 53.78%, 52.32% and 58.85%, and multi-position match accounted for 25.79%, 27.53% and 23.42%, respectively (Table 2).

Screening of differentially expressed genes and GO enrichment analysis results: Through the comparison of the expression differences of the three transcriptomes (F0, F1, F2), a total of 23720 differentially expressed genes were obtained (Figure 1). Among them, F0 vsF1 has the least number of differential genes, with 4039 up-regulated genes and 4313 down-regulated genes. In F0 vsF2, there are 6893 up-regulated genes and 9710 down-regulated genes. F1 vs F2, F1 has 7118 up-regulated genes and 10326 down-regulated genes.

GO function enrichment analysis showed that the most enriched differential genes in the three comparisons were F1vs F2, followed by F0 vs F2, and F0 vs F1 (Figure 2). In biological process, the most differentially expressed genes in the three comparisons were metabolic process, cellular process, and single-

organism process. In cellular component, cell, cell part and organelle were significantly enriched in the three comparisons, with equal numbers of cell and cell part. In the molecular function, the catalytic activity and the binding are much larger than the other functions in the three comparisons.

Results of KEGG functional analysis of differentially expressed genes: KEGG function analysis showed that 51439523 and 9924 differentially expressed genes were located on 347349 and 354 KEGG pathways in F0 vs F1, F0 vs F2 and F1 vs F2, respectively (Table 3). Among all the pathways, metabolic pathways are most significantly enriched, with annotation percentages of 24.03 %, 22.77 % and 22.82 %, respectively. The second is the biosynthesis of secondary metabolites pathways, with the annotation percentages of 14.58 %, 13.15 % and 13.23 %, respectively. The third is microbial metabolism in diverse environments. The growth and development of orchids are highly dependent on endophytic fungi, and microbial metabolism in diverse environments are significantly enriched during flower formation, indicating that *C. kanran* flowering may also be related to symbiotic microorganisms.

Screening of flowering-related genes: Among these differentially expressed genes, 29 homologous genes involving key genes for flowering regulation of *Arabidopsis* were found, and the expression of these genes was statistically analyzed (Table 4). Among the 29 genes, *CkFPA* is the homologous gene found in the spontaneous pathway, and *CkGA2OX*, *CkGID1*, *CkGA20OX* and *CkGA3OX* are four homologous genes found in the gibberellin pathway. Thirteen homologous genes including *CkGI*, *CkPHYA*, *CkPHYB*, *CkCRY*, *CkCRY1*, *CkCRY2*, *CkUVR8*, *CkCCA1*, *CkLHY*, *CkDOF5*, *CkFKF1* and *CkELF3* were found in the photoperiodic pathway. In the vernalization pathway, five homologous genes were compared, namely *CkVIN3*, *CkVRN*, *CkELF4*, *CkFRI* and *CkFLC*. The floral integron genes are *CkFT*, *CkSOC1*, *CkAP1*, *CkAGL6-2*, *CkAGL6-1* and *CkAGL8*, respectively.

Table 2. Comparison statistics of clean reads with reference genes

Sample	Total Reads	Total Mapped Reads (%)	Unique Match (%)	Multi-position Match (%)	Total Unmapped Reads (%)
F0	23625162	79.57	53.78	25.79	20.43
F1	22767464	79.85	52.32	27.53	20.15
F2	23948875	82.27	58.85	23.42	17.73

Note: F0: flower bud initiation stage, F1: flower primordium differentiation stage, F2: flower bud formation stage

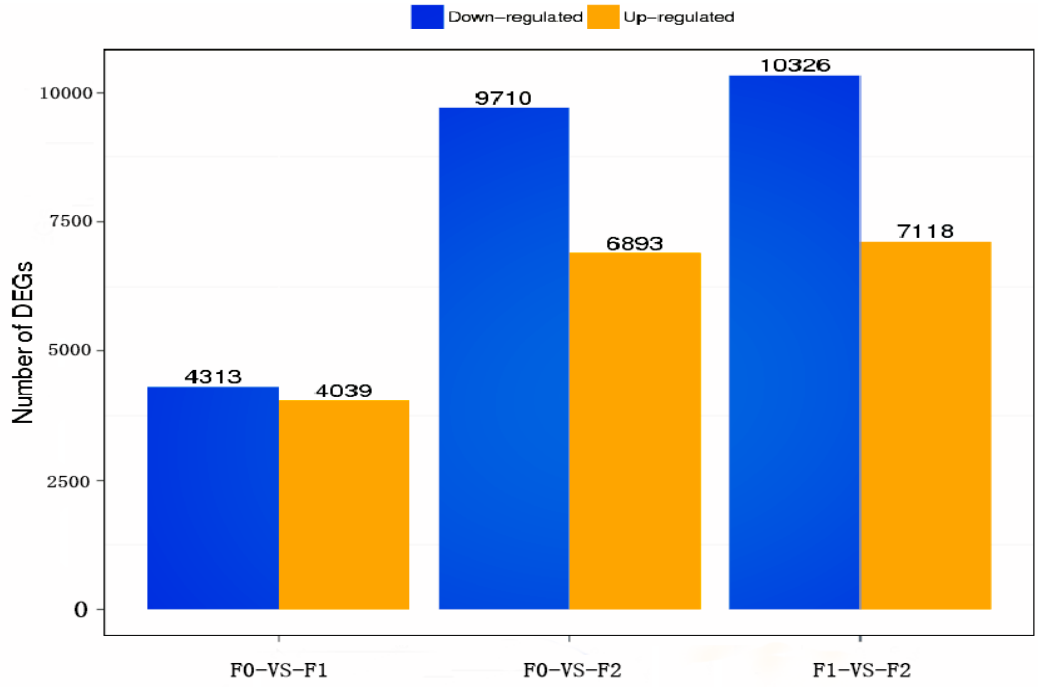

Figure 1. Comparison of the gene expression profile among F0, F1 and F2

Note: F0: flower bud initiation stage, F1: flower primordium differentiation stage, F2: flower bud formation stage

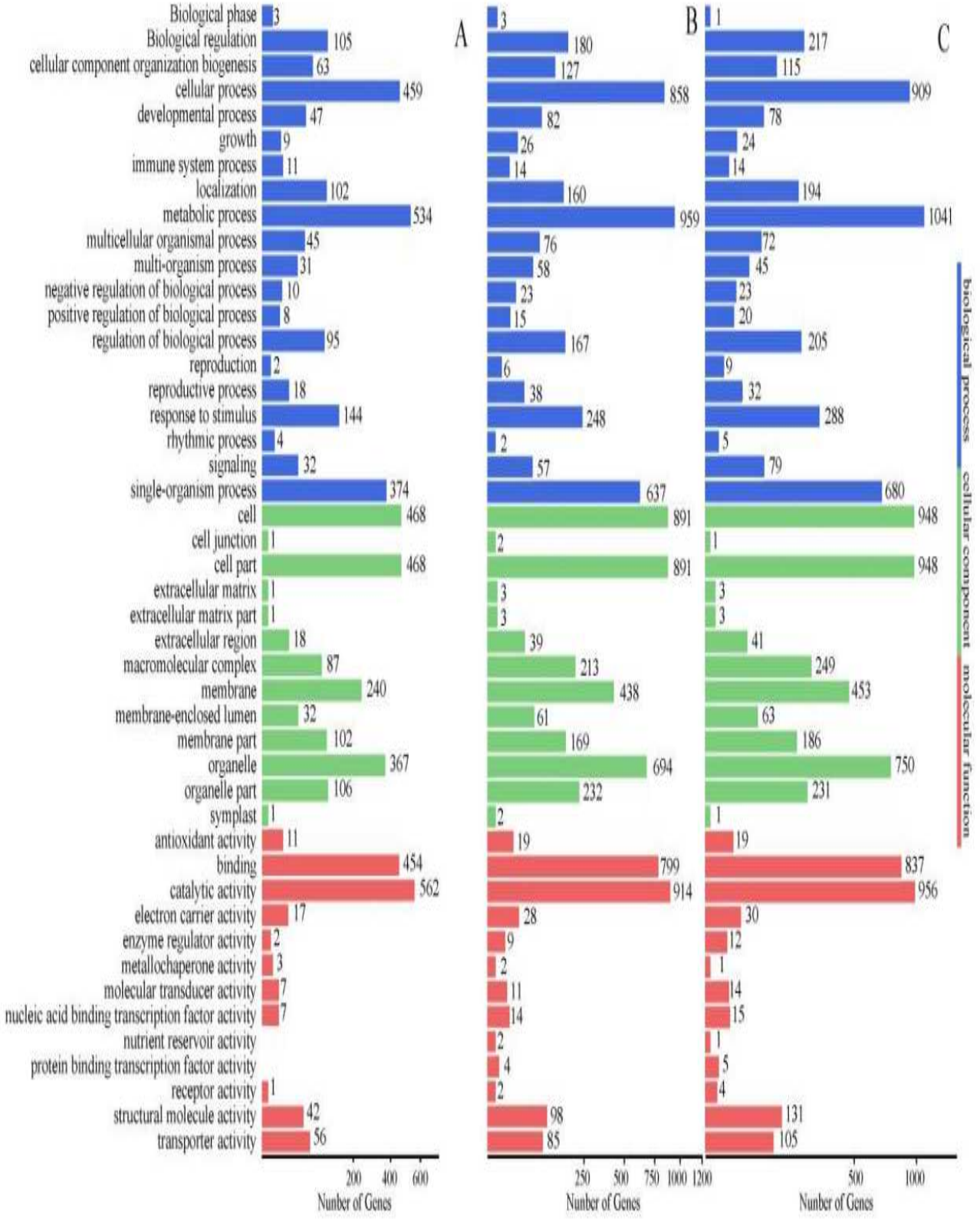

Figure 2. Results of Go function annotation for DEGs

Note: A: F0 vs F1; B: F0 vs F2; C: F1 vs F2 F0: flower bud initiation stage, F1: flower primordium differentiation stage, F2: flower bud formation stage

Table 3. The pathway analysis of DEGs in different flower buds

Pathway	The percentage of DEGs genes with pathway annotation (%)		
	F0-vs-F1	F0-vs-F2	F1-vs-F2
Metabolic pathways	24.03	22.77	22.82
Biosynthesis of secondary metabolites pathways	14.58	13.15	13.23
Microbial metabolism in diverse environments	4.57	4.12	4.36
RNA transport	4.30	4.89	4.57
Endocytosis	4.10	3.98	3.85
Epstein-Barr virus infection	4.01	4.37	4.26
Tuberculosis	3.97	3.87	3.81
Toxoplasmosis	3.64	3.57	3.39
Phenylpropanoid biosynthesis	3.62	2.94	2.81
Plant hormone signal transduction	3.54	3.03	3.12
Starch and sucrose metabolism	3.40	3.65	3.69
Leishmaniasis	3.23	2.95	2.84
Toll-like receptor signaling pathway	3.21	2.98	2.88
Apoptosis	3.15	3.00	2.93
Plant-pathogen interaction	2.88	3.05	3.03
Ribosome	2.24	3.43	3.83
Photosynthesis - antenna proteins	0.12	0.18	0.16

Note: F0: flower bud initiation stage, F1: flower primordium differentiation stage, F2: flower bud formation stage

Table 4. Putative 29 genes identified from DEGs associated with floral induction

Gene	Gene ID	FPKM in F0 F0 vs F1	FPKM in F1 F0 vs F2	FPKM in F2 F1 vs F2
Autonomic pathway				
CkFPA	CL3958.Contig2	3.04±0.18	0.59±0.04	6.28±0.33
		-2.37±0.14	1.05±0.05	3.41±0.10
Gibberellin pathway				
CkGA2OX	CL293.Contig1	0	6.98±0.40	2.37±0.15
		9.45±0.40	1.05±0.04	-1.56±0.05
CkGID1	CL7129.Contig1	3.6±0.22	0.95±0.03	21.74±0.78
		-1.92±0.09	2.59±0.14	4.52±0.16
CkGA20OX	Unigene11847	34.15±1.90	27.75±1.55	111.84±4.73
		-0.3±0.01	1.71±0.08	2.01±0.07
CkGA3OX	CL5408.Contig2	7.12±0.35	45.92±1.66	4.03±0.25
		2.69±0.12	-0.82±0.04	-3.51±0.11
Photoperiod pathway				
CkCO	CL380.Contig1	0	0	2.26±0.12
		-	7.82±0.28	7.82±0.40
CkGI	CL3290.Contig5	9.21±0.36	19.22±1.01	12.84±0.82
		1.06±0.05	0.48±0.03	-0.58±0.04
CkPHYA	CL3673.Contig1	2.05±0.14	4.46±0.15	3.22±0.16
		1.12±0.06	0.65±0.04	-0.47±0.02
CkPHYB	Unigene29242	26.73±1.09	1.52±0.06	57.44±1.95
		-4.14±0.28	1.1±0.06	5.24±0.29
CkCRY	Unigene37021	1.11±0.05	0	15.14±0.80
		-6.79±0.24	3.77±0.18	10.56±0.72
CkCRY1	Unigene14039	170.18±5.31	67.6±3.96	52.74±1.65
		-1.33±0.07	-1.69±0.08	-0.36±0.01
CkCRY2	CL2100.Contig1	5.27±0.18	2.23±0.15	0.21±0.01
		-1.24±0.07	-4.65±0.23	-3.410.22
CkUVR8	CL1477.Contig1	0	5.63±0.22	0.4±0.02

		9.14±0.30	5.32±0.16	-3.82±0.23
CkCCA1	CL1252.Contig1	0	4.58±0.26	4.49±0.24
		8.84±0.59	8.81±0.46	-0.03±0.00
CkLHY	CL4593.Contig1	0	1.87±0.13	2.31±0.16
		7.55±0.52	7.85±0.34	0.3±0.02
CkDOF5	Unigene9484	12.24±0.51	4.58±0.25	5.35±0.23
		-1.42±0.07	-1.19±0.05	0.22±0.01
CkFKF1	Unigene21256	3.91±0.14	4.65±0.16	0
		0.25±0.02	-8.61±0.42	-8.86±0.53
Ck×10LF3	CL7804.Contig2	1.38±0.04	18.89±0.80	0
		3.77±0.18	-7.11±0.25	-10.88±0.54
Vernalization pathway				
CkVIN3	Unigene39201	0.37±0.01	2.29±0.10	6.31±0.21
		2.63±0.16	4.09±0.20	1.46±0.04
CkVRN	Unigene8400	18.18±1.14	27.71±0.98	40.5±2.24
		0.61±0.02	1.16±0.05	0.55±0.03
Ck×10LF4	CL4422.Contig2	25.25±1.10	49.11±2.15	7.31±0.24
		0.96±0.03	-1.79±0.12	-2.75±0.13
CkFRI	CL5034.Contig3	25.45±1.02	4.79±0.29	87.55±4.64
		-2.41±0.11	-2.04±0.14	4.19±0.22
CkFLC	Unigene45600	12.28±0.64	6.13±0.23	2.99±0.20
		-1±0.07	-2.04±0.10	-1.04±0.06
Flowering integron				
CkFT	CL7224.Contig1	4.98±0.24	0	5.43±0.23
		-8.96±0.57	0.12±0.01	9.08±0.58
CkSOC1	Unigene6189	1.73±0.07	3.26±0.22	6.33±0.37
		0.91±0.06	1.87±0.11	0.96±0.03
CkAP1	Unigene1554	12.84±0.82	35.03±1.94	0.69±0.05
		1.45±0.09	-4.22±0.18	-5.67±0.22
CkAGL6-2	Unigene3794	6.23±0.39	3.9±0.26	13.74±0.64
		-0.68±0.04	1.14±0.05	1.82±0.11
CkAGL6-1	Unigene3318	3.64±0.20	0	0.94±0.03
		-8.51±0.50	-1.95±0.11	6.55±0.31
CkAGL8	CL3071.Contig2	4.06±0.24	5.49±0.36	2.23±0.10
		0.44±0.03	-0.86±0.06	-1.3±0.06

Note: F0 vs F1: log2 gene expression level in F0 compared to F1; a FDR (false discovery rate) < 0.001 and $|\log_2 Ratio| \geq 1$ indicates a significant difference.

qRT-PCR detection results of differentially expressed genes: In order to verify the accuracy of DEGs comparison in the flowering process of *C. kanran*, among the five types of flowering genes, the top two genes with the highest gene expression difference in each type were selected, and the gene expression amount was verified by qRT-PCR. There are 9 genes, including *CkFPA*, *CkGA2OX*, *CkGID1*, *CkCO*, *CkPHYB*, *CkELF3*, *CkFRI*, *CkFLC* and *CkAP1*. Comparing RNA seq and RT-qPCR data, it was found that the changes of all gene expression were not completely consistent, but the upward and downward trends of these genes were consistent in the three flowering stages (Figure 3A&B). In order to further verify the correlation between RNA-seq and RT-qPCR results, Pearson correlation coefficient analysis was performed on the results of both. Pearson correlation coefficient is R=0.728, indicating that the data obtained from the two analyses are highly significant positive correlation, which further reflects that the relative expression amount of genes obtained by RNA seq analysis is accurate and reliable, and it also proves that these 9 genes involved in the flowering pathway are differentially expressed during flowering in *C. kanran*, and these DEGs are likely to directly or indirectly affect the regulation of the flowering time in *C. kanran* (Figure 3C).

A: Gene expression data obtained through RNA-seq analysis; B: qRT-PCR analyses of gene expression ratios; Blue box: gene expression changes between F0 and F1; Red box: gene expression changes between F0 and F2; Green box: gene expression changes between F1 and F2; X-axis: genes; Y-axis: the fold change of the gene ($\log_2$ values); C: Pearson correlation analysis of the gene expression ratios obtained from the RNA-seq and the qRT-PCR data. X-axis: RNA-seq $\log_2$ values; Y-axis:

qRT-PCR log_2 values; R: the Pearson correlation coefficient; **: the extreme significant difference.

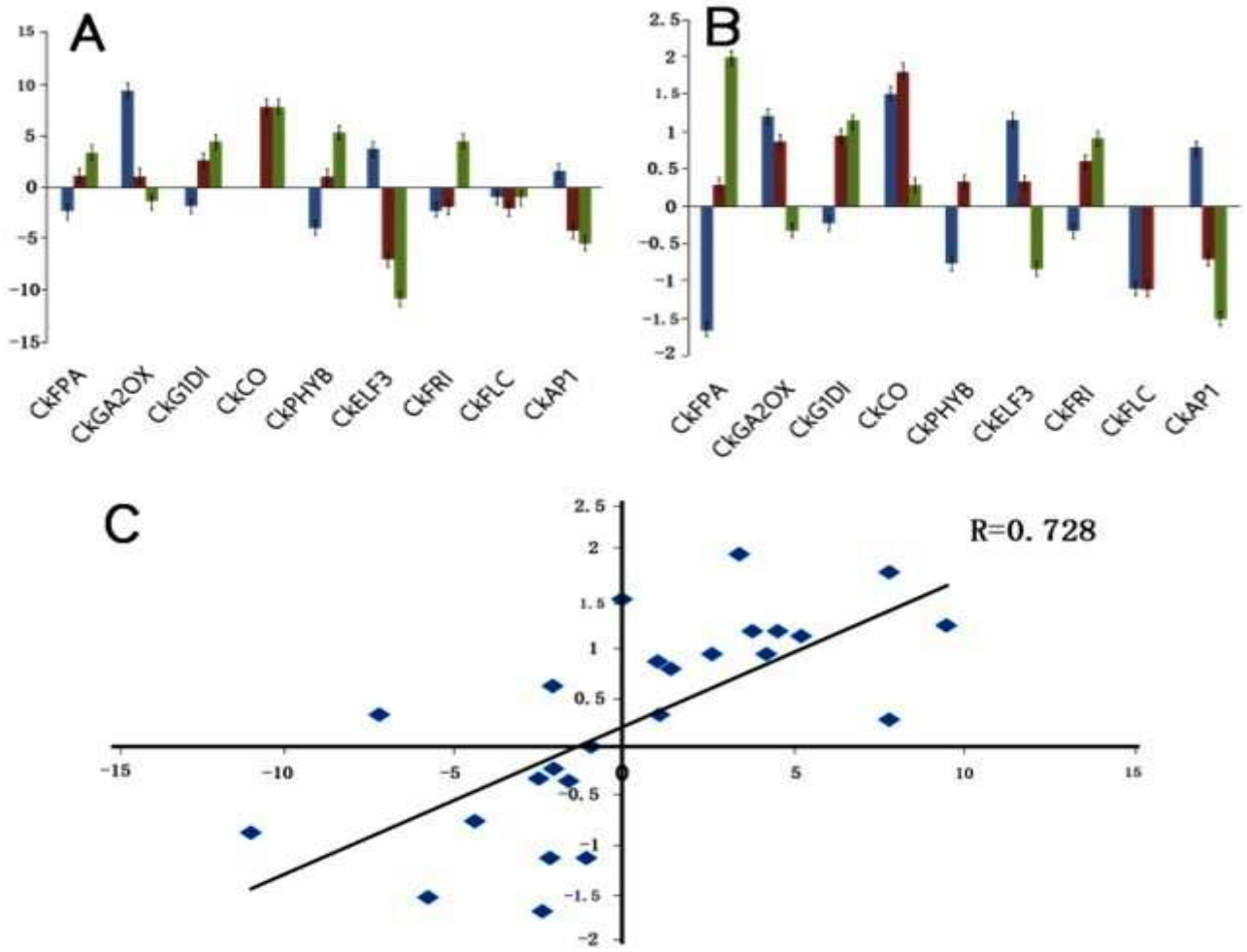

Figure 3. Identification of gene expression at different flowering stages

DISCUSSION

The juvenile period of *C. kanran* is relatively long, typically requiring 5-7 years to reach flowering, significantly limiting related studies and resource development for the flower development of *C. kanran* (Tsuji and Kato, 2010). This chapter laid a solid foundation for further unraveling the molecular mechanisms of *C. kanran* flowering by conducting DGE sequencing analysis on the flower buds at the stages of flower bud differentiation initiation, flower structure perfection, and flowering.

Three transcriptome databases, F0, F1, and F2, were obtained through high-throughput sequencing, with total reads of 23625162, 22767464, and 23948875, respectively. Comparative analysis of the expression differences among the three transcriptomes revealed a total of 23720 DEGs. The number of DEGs in F0 vs F1 was lower than in F0 vs F2 and F1 vs F2, reflecting the incomplete organ differentiation and imperfect flower structure in F0 and F1, leading to fewer differentially expressed genes. Further enrichment analysis of these DEGs through GO and KEGG showed significant enrichment in F0 vs F1, with the majority enriched in F0 vs F2 and F1 vs F2, indicating closer biological processes and metabolic pathways between F0 and F1, while F2 involved distinct biological processes and metabolic pathways compared to F0 and F1. By analyzing all DEGs and screening for homologous genes related to the flowering pathway in *Arabidopsis*, nine crucial DEGs were identified: *CkFPA*, *CkGA2OX*, *CkGID1*, *CkCO*, *CkPHYB*, *CkELF3*, *CkFRI*, *CkFLC*, and *CkAP1*. Validation using RT-qPCR and Pearson correlation coefficient analysis demonstrated a highly significant correlation between RT-qPCR and DEGs results, confirming the reliability of the DGE sequencing analysis. To further validate the roles of these nine DEGs in *C. kanran* flowering, RT-qPCR was employed to analyze their expression patterns throughout the entire

flowering process, aiming to elucidate their relationships with *C. kanran* flowering.

Plant flowering is regulated by a highly complex signal network, with light being a particularly crucial environmental signal factor. In *A. thaliana*, the key gene *CO* in the photoperiodic pathway is induced by long days, upregulating the expression of the *FT* gene, allowing *Arabidopsis* to flower under extended daylight (Yoo *et al.,* 2005; Wigge, 2006). In *C. kanran*, light also plays a significant role in the regulation of flowering time, and flower bud differentiation and flowering require light induction. The *CkCO* gene accumulates during the flowering induction period, with no expression during the flower bud differentiation initiation and flower structure perfection stages. The upregulation of this gene coincides with the period of bud germination and growth before flowering in *C. kanran*, suggesting that *CkCO* may promote the flower bud differentiation leading to *C. kanran* flowering. Additionally, KEGG enrichment analysis of differentially expressed genes during the induction period also indicated significant enrichment in photosynthesis in F0 vs F1, F0 vs F2, and F1 vs F2, indicating notable differences in the photosynthesis system during the three flowering stages. Therefore, light, acting on the flowering process of *C. kanran*, plays a more crucial role in F2 compared to F0, with the high expression of *CO* potentially inducing *C. kanran* flowering. Previous studies have also suggested that sustained overexpression of *CO* can rapidly induce flowering in plants under non-inductive conditions (Putterill *et al.,* 2004). Simultaneously, *PHYB* perceives red and far-red light, acting as a light receptor sensing day length and night length, generating circadian rhythms. *ELF3* is a gene influencing circadian rhythms, and light regulates flowering time through the circadian clock by transmitting the signal of day length to *CO*, inducing the downstream expression of the *FT* gene, thereby promoting plant flowering (Hui *et al.,* 2011). Therefore, in this study, *CkCO* is a valuable gene that likely induces *C. kanran* flowering and deserves further investigation.

The genes associated with flowering in the endogenous pathway operate independently of genes in other pathways, unaffected by their regulatory mechanisms. *FPA* functions to promote flowering by inhibiting the expression of the *FLC* gene and enhancing gibberellin synthesis (Fan, 2014). *CkFPA* exhibits significantly elevated expression levels during the stages of flower bud differentiation initiation, flower organ perfection, and flowering, suggesting its potential involvement in the induction of *C. kanran* flowering.

In *Arabidopsis*, vernalization refers to the induction of flowering by low temperatures, and a similar process exists in perennial herbaceous plants, where low temperatures are linked to flowering (Tang *et al.,* 2007). Exposure to low temperatures before flowering can advance the flowering period, as seen in *C. kanran*, where low-temperature treatment during flower bud differentiation initiation can hasten flowering. The low expression of *CkFLC*, consistent with the inhibitory role of high-level *FLC* expression in flowering in *Arabidopsis* mutant studies, indicates a correlation between *CkFLC* and *C. kanran* flowering. The high expression of *CkFRI* during the flower bud differentiation initiation and flowering induction stages suggests that *CkFRI* may inhibit flower bud differentiation and flowering in *C. kanran*. In *Arabidopsis*, *FRI* is a key gene influencing flowering time, delaying flowering by promoting the expression of the flowering inhibitor *FLC*136 (Clarke and Dean, 1994). Therefore, *CkFLC* may play an inhibitory role in the induction of *C. kanran* flowering.

Numerous studies have highlighted the crucial influence of gibberellin on the flowering process in plants, with apparent species specificity. In *Arabidopsis*, gibberellin promotes flowering induction (Fan, 2014). In this study, genes *CkGA2OX* and *CkGID1* exhibited differential expression during all three flowering induction stages, suggesting a potential role for gibberellin in promoting flowering induction in *C. kanran*. The significantly higher expression level of *CkGID1* during the flowering induction stage compared to the first two stages is similar to the feedback mechanism of *GID1* in the gibberellin pathway observed in *Arabidopsis* and rice (Gomi, *et al*., 2004; Hartweck and Olszewski, 2006; Griffiths, *et al*., 2006). *CkGA2OX*, with no expression during the flower bud differentiation initiation stage but significantly increased expression during the flower organ perfection and flowering stages, indicates the potential involvement of gibberellin in the induction of *C. kanran* flowering. Gibberellin can break dormancy, reduce the temperature accumulation requirement for flowering, and accelerate the appearance of orchid flower primordia, suggesting that *CkGA2OX* may play a crucial regulatory role in promoting the early flowering of *C. kanran*.

Floral integrators combine multiple flowering pathways to induce the expression of downstream floral organ genes, determining the plant's flowering time (Li *et al.,* 2014). In this study, *CkAP1* exhibited a significant initial increase in expression during all three stages of *C. kanran* and a subsequent significant decrease during the flowering stage, implying its crucial role in flower organ perfection. This finding aligns with the early discovery that *AP1* is a necessary floral organ development gene (Kunst *et al.,* 1989). Once floral initiation reaches the flower structure perfection stage, flowering becomes irreversible, further indicating that *CkAP1* plays a promotive role in *C. kanran* flowering.

In *Arabidopsis*, flowering is primarily induced and regulated through the photoperiod pathway, vernalization pathway, autonomous pathway, and gibberellin pathway. In this study, through DEGs

comparison during the flowering induction stage, it was evident that key genes in all four pathways exhibited differential expression, highlighting the complexity of the flowering regulation mechanism in *C. kanran*. Further analysis of the expression patterns of these differentially expressed genes revealed a significant upregulation of *CkFPA*, *CkGA2OX*, and *CkCO* during the flower bud growth process. The synchronized expression patterns of these three genes, opposite to that of *CkFLC*, signify their roles as key genes in the autonomous, gibberellin, and photoperiod pathways, respectively. The coupled expression of the floral integrator *CkAP1* with these key genes implies that the flowering of *C. kanran* is co-regulated by the autonomous, gibberellin, photoperiod, and vernalization pathways. Techniques such as temperature regulation (vernalization pathway), light exposure (photoperiod pathway), and external hormone application (GA3) could be employed in cultivation to modulate the flowering of *C. kanran* based on external environmental factors.

Conclusion: This study conducted high-throughput sequencing during the flower primordium differentiation period, flower structure maturation period, and flowering period of *C. kanran*, resulting in three transcriptome databases with total reads of 23625162, 22767464, and 23948875, respectively. DGE analysis and RT-qPCR validation were performed on 23720 differentially expressed genes identified from the three transcriptomes, leading to the identification of nine differentially expressed genes related to *C. kanran* flowering: *CkFPA*, *CkGA2OX, CkGID1*, *CkCO*, *CkPHYB*, *CkELF3, CkFRI*, *CkFLC*, and *CkAP1*. This discovery establishes the foundation for regulating the flowering time of *C. kanran*, significantly advancing research on flower development in *C. kanran* and other orchidaceous plants, and promoting resource development.

Acknowledgements: We thank Jiangxi Provincial Key Laboratory of Plant Resources for providing us *Cymbidium kanran* as experimental materials.

Author contributions: LHL and YBY conceived and designed the study. LWY performed experiments. LWY, LSF and WXC analyzed data. LWY wrote the manuscript. LSF prepared figures and tables. All authors read and approved the final manuscript.

Funding: This work was supported by the National Natural Science Foundation of China (Grant No. 32160720) and Open Foundation for Key Laboratory of National Forestry and Grassland Administration for Orchid Conservation and Utilization (Grant No. OC202101).

Disclosure statement: The authors declare that they have no competing interest.

Data availability statement: The RNA-seq data for all organization without treatment. The accession is PRJNA533480.

REFERENCES

Andres, F and G. Coupland (2012). The genetic basis of flowering responses to seasonal cues. *Nat. Rev. Gen.* 2012, 13(9): 627-639. https://doi.org/10.1038/nrg3291

Blümel, M., N. Dally and C. Jung (2015). Flowering time regulation in crops - what did we learn from *Arabidopsis*? *Curr. Opin. Biotechnol.* 32: 121-129. https://doi.org/10.1016/j.copbio.2014.11.023

Clarke J. H. and C. Dean (1994). Mapping *FRI*, a locus controlling flowering time and vernalization response in *Arabidopsis thaliana*. *Mol. Genet. Genomics* 242(1): 81-89. https://doi.org/:10.1007/BF00277351

Contil, L (2017). Hormonal control of the floral transition: can one catch them all? *Dev. Biol.* 430(2): 288-301. https://doi.org/10.1016/j.ydbio.2017.03.024

Crane, O., T. Halaly, X. Q. Pang, S. Lavees, A. Perl and R. Vankova (2012). Cytokinin-induced VvTFL1A expression may be involved in the control of grapevine fruitfulness. Planta. 235(1): 181-192. https://doi.org/10.1016/j.ydbio.2017.03.024

Chen, X. L., S. Y., Qi, D. Zhang, Y. M. Li, N. An, C. P. Zhao, J. Zhao, K. Shan, M. Y. Han and L. B. Xing (2018). Comparative RNA-sequencingbased transcriptome profiling of buds from profusely flowering 'Qinguan' and weakly flowering 'Nagafu no. 2' apple varieties reveals novel insights into the regulatory mechanisms underlying floral induction. *BMC Plant Biol.* 18(1): 370. https://doi.org/10.1186/s12870-018-1555-3

Chen, Y. H., J. H. Chen and Y. M. Luo (2012). Complementary biodiesel combination from tung and medium-chain fatty acid oils. *Renew. Energ.* 44: 305-310. https://doi.org/10.1016/j.renene.2012.01.098

Cui, Z., B. Zhou, Z. Zhang and Z. Hu (2013). Abscisic acid promotes flowering and enhances *LcAP1* expression in Litchi chinensis Sonn. *S. Afr. J. Bot.* 88: 76-79. https://doi.org/10.1016/j.sajb.2013.05.008

Díaz-Riquelme, J., J. M. Martínez-zapater and M. J. Carmona (2014). Transcriptional analysis of tendril and inflorescence development in grapevine (*Vitis vinifera* L.). *PLoS ONE.* 9(3): e92339. https://doi.org/10.1371/journal.pone.0092339

Fan, S.G (2014). Advances in molecular mechanism of floral formation in higher plants. *J. Chuxiong Nor Uni*. 29(06): 58-69. https://api.semanticscholar.org/CorpusID:87874810

Feng, J. Q., Q. Xia, F. P. Zhang, J. H. Wang and S. B. Zhang (2021). Is seasonal flowering time of *Paphiopedilum* species caused by differences in initial time of floral bud differentiation? *AoB Plants.* 20;13(5): plab053. https://doi.org/10.1093/aobpla/plab053

Ferrandiz, C., Q. Gu, R. Martienssen and M. F. Yanofsky (2000). Redundant regulation of meristem identity and plant architecture by *FRUITFULL*, *APETALA1* and *CAULIFLOWER*. *Neuropathol*. 127(4): 725-734. https://doi.org/10.1242/dev.127.4.725

Fornara, F., A. De Montaigu and G. Coupland (2010). SnapShot: Control of flowering in *Arabidopsis*. *Cell*. 2010, 141(3): 550. https://doi.org/10.1016/j.cell.2010.04.024

Gomi, K., A. Sasaki, H. Itoh, M. Ueguchi-Tanaka, M. Ashikari, H. Kitano and M. Matsuoka (2004). *GID2*, an F-box subunit of the SCF E3 complex, specifically interacts with phosphorylated SLR1 protein and regulates the gibberellin-dependent degradation of SLR1 in rice. *Plant J.* 37(4): 626-634. https://doi.org/10.1111/j.1365-313x.2003.01990.x

Griffiths, J., K. Murase, I. Rieu, R. Zentella, Z. L. Zhang, S. J. Powers, F. Gong, A. L. Phillips, P. Hedden, T. P. Sun and S. G. Thomas (2006). Genetic characterization and functional analysis of the GID1 gibberellin receptors in *Arabidopsis. Plant Cell* 19(2): 726-726. https://doi.org/10.1105/tpc.106.047415

Hartweck, L. M and N. E. Olszewski (2006). Rice GIBBERELLIN INSENSITIVE DWARF1 is a gibberellin receptor that illuminates and raises questions about GA signaling. *Plant Cell* 18(2): 278-282. https://doi.org/10.1105/tpc.105.039958

Hui, J., C. L. Huang, Z. Y. Wu and X. H. Zhang (2011). Study on the transformation of *Arabidopsis thaliana* photosensitive pigment genes *PHYA* into *Chrysanthemum*. *Jiangsu Agr. Sci.* 39(2): 51-54. https://doi.org/10.3969/j.issn.1002-1302.2011.02.015

Huang, S. L., Y. C. Qiao, X. M. Lv, J. G. Li, D. M. Han and D. L. Guo (2022). Transcriptome sequencing and DEG analysis in different developmental stages of floral buds induced by potassium chlorate in *Dimocarpus longan*. *Plant Biotechnol.* 39: 259–272. https://doi.org/10.5511/plantbiotechnology.22.0526a

Jeong, K.M., M. Yang, Y. Jin, E.M. Kim, J. Ko and J. Lee (2017). Identification of major flavone C-Glycosides and their optimized extraction from *Cymbidium kanran* using deep eutectic solvents. *Molecules.* 22(11): 11. https://doi.org/10.3390/molecules22112006

Jian, L and I. Q. Zhu (2010). Analysis on *Cymbidium kanran* with SRAP markers. *Sci. Agr. Sin.* 43(15): 3184-3190. https://doi.org/10.3864/j.issn.0578-1752.2010.15.016

Jiang X. F. (2007). Study on morphologic anatomy of *Cymbidium kanran* Makino in vitro flowering. Nanchang University. https://doi.org/10.7666/d.y1814350

Jing, D., W. Chen, R. Hu, Y. Zhang, Y. Xia, S. Wang, Q. He, Q. Guo and G. Liang (2020). An integrative analysis of transcriptome, proteome and hormones reveals key differentially expressed genes and metabolic pathways involved in flower development in loquat. Intern. *J. Mol. Sci.* 21(14): E5107. https://doi.org/10.3390/ijms21145107

Kunst L., J. E. Klenz, J. Martinez-Zapater and G.W Haughn (1989). *AP2* Gene Determines the Identity of Perianth Organs in Flowers of *Arabidopsis thaliana*. *Plant Cell.* 1(12): 1195-1208. https://doi.org/10.1105/tpc.1.12.1195

Li J., H. Y. Gu, Z. M. Wang, Q. L. Tang and M. Song (2014). Research progress of flowering gene regulatory networks in *Arabidopsis thaliana*. *Biotechn. Bulletin.* (12): 1-8. https://doi.org/10.13560/j.cnki.biotech.bull

Lin, L., Y. Huang, T. L. Xie, Y. Zhang, Y. M. Zhou and R. D. Wen (2012). Changes of endogenous hormone content during flower bud differentiation in three grape varieties. *J. Southern Agr.* 43(6): 806-809. https://doi.org/10.3969/j:issn.2095-1191.2012.06

Liu, D., X. Sun, X. Mu, W. M. Wu, Z. Zhang and J. G. Fang (2015). Analysis of expression levels of floral genes in the buds on different branch nodes of grapevine. *Sci. Agr. Sin.* 48(10): 2007-2016. https://doi.org/10.3864/j.issn.0578-1752.2015.10.013

Putterill, J., R. Laurie and R. Macknight (2004). It's time to flower: the genetic control of flowering time. *Bioessays.* 26(4): 363-373. https://doi.org/10.1002/bies.20021

Tang Q. L., X. J. Wang, M. Song, C. Q. Li and H. Zhang (2007). Vernalization-related genes and model of vernalization memeory in *Arabidopsis thaliana*. *Plant Physiol. Commun.* 43(05): 805-810. https://doi.org/10.1360/aps07042

Theißen, G., R. Meizer and F. Rümpler (2016). MADS-domain transcription factors and the floral

quartet model of flower development: linking plant development and evolution. *Develop*. 143(18): 3259-3271. https://doi.org/10.1242/dev.134080

Tsuji, K. and M. Kato (2010). Odor-guided bee pollinators of two endangered winter/early spring blooming orchids, *Cymbidium kanran* and *Cymbidium goeringii*, in Japan. *Plant Spec. Biol.* 25(3): 249-253. https://doi.org/10.1111/j.1442-1984.2010.00294.x

Wang, H. B., J. Q. Zhao, X. D. Wang, X. B. Shi, B. L. Wang, X. C. Zheng and F. Z. Liu (2014). The influence of changes of endogenous hormones in shoot on the grapes flower bud differentiation in greenhouse. *Sci. Agri. Sin.* 47(23): 4695-4705. https://doi.org/10.1007/s00402-014-2015-7

Wigge, P. A (2006). Integration of spatial and temporal information during floral induction in *Arabidopsis*. *Sci.* 312(5780): 1600-1600. https://doi.org/10.1126/science.1114358

Wilhelm, B. T. and J. R. Landry (2009). RNA-Seq-quantitative measurement of expression through massively parallel RNA-sequencing. *Methods.* 48(3): 249-257. https://doi.org/10.1016/j.ymeth.2009.03.016

Yamaguchi, N., M. F. Wu, C. M. Winter and D. Wagner (2014). LEAFY and polar auxin transport coordinately regulate *Arabidopsis* flower development. *Plants.* 3(2): 251-265. https://doi.org/10.3390/plants3020251

Yoo, S. K., K. S. Chung, J. Kim, J. H. Lee, S. M. Hong, S. J. Yoo, S. Y. Yoo, J. S. Lee and J. H. Ahn (2005). CONSTANS activates SUPPRESSOR OFOVEREXPRESSION OFCONSTANS 1 through FLOWERING LOCUS T to promote flowering in *Arabidopsis*. *Plant Physiol.* 139(2): 770-778. https://doi.org/10.1104/pp.105.066928

Yu, H and C.J. Goh (2001). Molecular genetics of reproductive biology in orchids. *Plant. Physiol.* 127(4): 1390-1393. https://doi.org/10.1104/pp.010676

Zhu G. B., B. Y. Yang and A. Y. Ao (2008). Tissue culture and in vitro flowering of *Cymbidium kanran* Makino. *Plant Physiol. Comm.* (03): 513-514+141. https://doi.org/10.13592/j.cnki.ppj.2008.03.050

Zou, L. P., C. Pan, M. X. Wang, L. Cui and B. Y. Han (2020). Progress on the mechanism of hormones regulating plant flower formation. *Hereditas*. 42(8): 739-751. https://doi.org/10.16288/j.yczz.20-014.